Antagonist softening and hardening effects of hydrogen investigated using nanoindentation on cyclically pre-strained nickel single crystal

G. Hachet, A. Oudriss, A. Barnoush, T. Hajilou, D. Wang, A. Metsue, X. Feaugas

Version of Record: https://www.sciencedirect.com/science/article/pii/S0921509320315434
Manuscript_144ced88c0b012d49cbfeaa6a24df31e

Antagonist softening and hardening effects of hydrogen investigated using nanoindentation on cyclically pre-strained nickel single crystal

G. Hachet[1,3*], A. Oudriss[1], A. Barnoush[2], T. Hajilou[2], D. Wang[2], A. Metsue[1] and X. Feaugas[1]

[1] La Rochelle University, LaSIE UMR CNRS 7356, Avenue Michel Crépeau, 17000 La Rochelle.
[2] Department of Mechanical and Industrial Engineering, Norwegian University of Science and Technology, Richard Birkelands vei 2b, 7491, Trondheim, Norway
[3] CEA Saclay, Service de Recherches de Métallurgie Physique, 91191, Gif-sur-Yvette, France
[*] Corresponding author: guillaume.hachet@gmx.com

Abstract: Since hydrogen-plasticity interaction is a key feature in the study of hydrogen embrittlement, a series of nanoindentation tests were carried out to evaluate the possible impact of hydrogen on the dislocation structures formed during cyclic pre-straining of nickel single crystal. *Ex-situ* nanoindentation and *in-situ* electrochemical nanoindentation tests were performed on cyclically pre-strained nickel single crystal and nickel-hydrogen systems to characterise the change in the reduced modulus and hardness. Although the reduced modulus was less affected by the conditions explored, the change in hardness highlights the competition between the hardening and softening processes associated with hydrogen. When hydrogen was pre-charged before the cyclic tests, the dislocation microstructures were softer than those induced by cyclic tests in hydrogen-free metals. In contrast, when *in-situ* electrochemical nanoindentation tests were performed, the hydrogen ingress on cyclically strained nickel single crystal induced a hardening of the microstructure. This effect was due to a pinning effect by the solute on the dislocations. The competition between these processes is discussed in terms of hydrogen and vacancy concentrations.

Keywords: Hydrogen, Vacancies, Nickel, Nanoindentation, Plasticity

1. Introduction

Hydrogen is a strong candidate for the development of alternative energies since it is a zero-emission fuel, but it also influences the mechanical properties of metals and alloys, inducing pre-mature failure [1,2]. Moreover, when hydrogen is introduced as a solute into nickel, it can transform a ductile fracture into a brittle fracture [3]. However, hydrogen solutes can also induce slip bands at damage surfaces, raising questions about the contribution of plasticity to the initiation of brittle fractures [4]. To describe this critical state, which is more commonly known as hydrogen embrittlement (HE), an explanation of damage initiation is needed. Different models have been proposed which are mostly based on a reduction of energy in the presence of the solute [5,6]; they are described in the following reviews: [7–10]. Although all the proposed models describe the interaction between hydrogen and microstructural defects such as dislocations and vacancies, HE is more complicated to describe when a metal is plastically strained since this involves managing a large variety of length and time scales for several mechanisms. When a metal is plastically strained (as a result of tensile stress or fatigue), it develops heterogeneities which vary with the plastic strain amplitude (γ_P). Different deformation "regimes", which are commonly called hardening stages, can be then observed as a function of the microstructure obtained [11–14]. These hardening stages correspond to the predominance of a particular dislocation structure and can be represented as a map (several maps are available in the literature for different FCC metals: [12,15]). When a metal is cyclically strained, it develops a dipolar microstructure of edge dislocations that first appear as veins in stage II_0 [12,16–18]. The hardening stage III_0 is reached at higher deformation amplitudes. At this stage, vein dislocation structures are reorganised in a ladder to form dipolar structures such as persistent slip bands (PSB) or labyrinth structures, depending on the orientation of the cyclic tests. The latter have a composite-like structure, displaying a wall phase with a high dislocation density and a channel phase with a low dislocation density [19,20]. Finally, the metal reaches stage III for large deformations and at high plastic strain amplitudes. At this level, the metal is severely deformed and develops different kinds of dislocation cells [21,22].

The effect of hydrogen on the mechanical response of strained (tensile) nickel single crystal oriented for single slip [23–26] and multiple slips [23,27] has been studied. It is clear that hydrogen can introduce

different softening and hardening effects on nickel single crystal depending on the plastic strain and the strain rate. When a metal is tensile strained, the presence of hydrogen induces a hardening at low deformation (shear strain $\gamma < 0.1$), which is mainly due to hydrogen in the Cottrell atmosphere increasing the drag stress of dislocations [26,27], an effect that is also observed in polycrystalline nickel [28,29]. A softening effect is observed when a metal is oriented for single and multi-slips at a higher plastic strain in the presence of hydrogen [26,27]. This consequence was noticed due to the shielding effect of the solute, which reduced the internal stress and induced a delay in the cross-slip events in dislocations [26,27]. As for cyclic deformation, a reduction in cyclic hardening was obtained for all hardening stages when a metal was pre-charged with hydrogen and oriented for single slip [30]. Moreover, the authors also noted that the formation of persistent slip bands occurred at higher plastic strain amplitudes, corresponding to a delay in cross-slip events [25,30]. This delay was also observed in cyclically strained nickel single crystals oriented for multi-slips, with a minor hardening due to hydrogen at higher plastic strain amplitudes [31]. When the dislocation structures induced by fatigue in the presence or absence of hydrogen were analysed over a smaller length, the solute was found to reduce the short-range interaction of dislocations, mostly in the channel phase (which contained low dislocation densities), in relation to the shielding process. However, the solute increased the long-range interaction induced by the wall phase at high dislocation densities (a phase that is mostly constituted of edge dislocation dipoles) in relation to the formation of the Cottrell atmosphere, which can be attenuated by the formation of vacancies and vacancy clusters [32]. In a previous study, we attempted to reproduce these results by employing a crystal plasticity model [33]. The results showed that hydrogen can promote hardening and softening effects through different mechanisms. Despite these studies, a difference in the effects of mobile and trapped hydrogen has not been clearly established.

Depending on the dislocation structures induced by fatigue in the presence or absence of hydrogen, a clear competition between hardening and softening is obtained. Hence, the use of nanoindentation (NI) is appropriate because it can be used to determine the hardness of a metal with and without hydrogen. NI has been performed with hydrogen pre-charged nickel alloys (Ni-201) and aged nickel alloy hydrogen systems [34]. In both cases, it was observed that hydrogen had a minor effect on hardness, but it decreased the reduced modulus in relation to the enhancement of vacancy formation by hydrogen incorporation. Moreover, *in-situ* electrochemical nanoindentation (ECNI) has been developed for different metals, including nickel and nickel alloys, improving the quantification of the impact of mobile hydrogen on physical properties [35–40]. When the solute is introduced electrochemically, it has been demonstrated in different metals that hardness increases (the maximum indent depths were lower during cathodic polarisation) [35,37–40], and also the reduced modulus decreases with hydrogen charging time [40]. This variation in hardness has been explained by the pinning of dislocations by the solute [38,39], which is supported by atomic and dynamic dislocation simulations representing the interaction between hydrogen and dislocation [32,41,42]. However, less information is available about these parameters when the sample is pre-strained. In this study we therefore proposed to perform NI on cyclically pre-strained nickel single crystal with and without hydrogen. The modification in hardness and the reduced modulus are discussed according to when hydrogen is incorporated (before or during indentation) and the dislocation structures induced by the cyclic tests.

2. Method

NI tests were performed on cyclically pre-strained nickel and nickel-hydrogen pre-charged systems to mechanically quantify the consequences of dislocation structures induced by cyclic tests in nickel crystal with and without hydrogen. **Table 1** presents the different samples used in this work. The details of the hydrogen incorporation and fatigue tests were described in a previous study [31]. All mechanical tests (tensile, fatigue and nanoindentation tests) were performed with the crystallographic <001> axis parallel to the normal direction of the samples. In addition, we performed NI tests on <001> oriented nickel single crystal without hydrogen and deformation, which were used as a reference for this study.

The same surface preparation was used for all samples. First, the extrema of the cyclically strained specimens were cut to obtain samples with a dimension of 6x4x1 mm^3. They were then coated in a Mecaprex MA2+ epoxy resin to form a cylinder 12 mm in diameter. The samples were electrochemically polished using Struers lectopol-4. Polishing was carried out at ambient temperature for 20 seconds at 30V in a solution 1M methanolic H_2SO_4 to limit the roughness as much as possible [35,37]. Sample surface roughness was verified

by scanning probe microscopy (SPM) on each sample after electropolishing. The NI tests were performed only when the surface roughness varied by a few nanometres on a 100 μm^2 surface using a TI 950 Hysitron triboindenter [38,39,43].

Table 1: Chosen samples for NI tests. The plastic shear strain amplitude (γ_p) with the corresponding hardening stage is provided for each sample. The nickel-hydrogen systems had an initial hydrogen concentration of 4×10^{-4} H/Ni (~7 wppm) and they were aged at room temperature over several months.

Configuration	Specimen number	Specimen number in [31]	γ_p	hardening Stage
Ni	A1	A4	2.5×10^{-4}	II_0
	A2	A7	14×10^{-4}	III_0
	A3	A8	25×10^{-4}	III_0/III transition
	A4	A10	51×10^{-4}	III
Ni-H	B1	B5	7.5×10^{-4}	II_0/III_0 transition
	B2	B9	20.5×10^{-4}	III_0/III transition
	B3	B11	32.5×10^{-4}	III

In-situ ECNI tests were then performed on cyclically strained nickel single crystal samples (sample numbers A1 and A4 on **Table 1**). The experimental set-up containing three electrodes (working-, reference- and counter-electrode) was connected to the cell through a double junction and used for *in-situ* testing in various studies [35,44]. The sample represents the working electrode, and hydrogen charging was carried out by applying a cathodic current density. For hydrogen desorption, an anodic potential was applied. Charging potential was measured using a $Hg/HgSO_4$ reference electrode [37,39]. Moreover, the solution used was a mixture of 80% borax/glycerol, 20% distilled water and 0.002 M sodium thiosulfate; the sulphate favours the absorption of the hydrogen in the sample. The first current density was -0.4 mA.cm^{-2}, corresponding to a potential between -2 V and -1.7 V to incorporate the solute. We then used an anodic potential of +100 mV to desorb hydrogen from the samples. A delay of 30 minutes between the beginning of the cathodic (and anodic) polarisation and the beginning of the NI tests was used, allowing hydrogen to be absorbed (and desorbed) to (from) the metal [37]. Finally, it should be noted that this charging procedure does not provide an evaluation of the charged or desorbed hydrogen concentration.

The tip and load function for the indentation tests were identical to the ones described in the previous study [31]. A 90° cube-corner shaped tip was chosen and the applied load function of each indentation consisted of a loading rate of 200μN.s^{-1} up to the maximum load F_{max}, which varied between 5 μN and 500 μN for the first NI tests. The maximum load was kept constant for 3 s in order to observe any creep effect during the loading [45], then it was reduced to 10% of the maximum load for 1.25 s for drift correction [37]. The feedback during testing was set to open-loop (no feedback). In this way, no feedback was used to control the load or the displacement during testing [46]. However, it is important to note the acquired maximum load P_{max} may be different from F_{max} in the obtained load-displacement (L-D) curves. Finally, we determined the hardness, H, and the reduced modulus, E_r, of the metal using the Oliver and Pharr method [47–49]:

$$H = \frac{P_{max}}{A_p} \tag{1}$$

and

$$E_r = \frac{\sqrt{\pi}}{2\sqrt{A_p}} \times \frac{dP}{dh} \tag{2}$$

where dP/dh is the experimentally measured stiffness from the upper portion of the unloading part of the L-D curves and A_p is the projected contact area evaluated from the contact depth (h_c) and the tip area function.

In order to improve our understanding of the antagonist softening and hardening effects of hydrogen and the contribution of vacancies, we performed additional experiments on unstrained nickel single crystal and nickel-hydrogen systems. Uniaxial tensile tests were conducted on nickel-hydrogen systems aged in air and oriented parallel to the <001> axis. The sample was electrochemically charged for 72 h before the tensile tests using the conditions presented in previous studies [50,51]. The initial hydrogen concentration was around 4.06×10^{-4} H/Ni, which was measured using thermal desorption spectroscopy (TDS). The mechanical tests were performed identically to those presented in the previous study (micro-tensile testing machine, Kammrath & Weiss 5 kN and a MTS 632.13F 10 mm extensometer [51]). With this set-up, we remained within the elastic regime of the metal for all tensile tests (*i.e*. the yield stress was less than 50 MPa with a strain rate of 2.10^{-5} s^{-1}) [52].

In parallel, we conducted TDS analyses on nickel-hydrogen systems having the same thickness as the tensile strained sample in the elastic domains and aged in the same condition in air. The TDS analyses were conducted with a Jobin Yvon Horiba EMGA-621W hydrogen analyser comprising a thermal conductivity detector (TCD) [53]. Moreover, to investigate the consequences of vacancies induced by the hydrogen insertion, we also quantified the vacancy concentration in aged nickel-hydrogen systems at several hydrogen desorption times using differential scanning calorimetry (DSC) [53,54]. The vacancy concentration C_{Vac} was determined through the stored energy of vacancies E_{Vac}^{st} obtained from the heat flow curves of the DSC. C_{Vac} was then calculated using the following equation [53,55]:

$$C_{Vac} = \frac{E_{Vac}^{st}}{e_{Vac}} \times \frac{N_A}{M_{Ni}} \tag{3}$$

where e_{Vac} is the formation energy of vacancies in nickel single crystal, which was 1.49 eV at 300 K according to *ab initio* calculations [56]. N_A and M_{Ni} are the Avogadro number and the molar mass of the host metal, respectively.

We first performed NI on cyclically pre-strained nickel single crystal and aged nickel hydrogen systems (the NI test performed on pure nickel without any deformation is given in supplementary material 1). The aim of this study was to understand how the incorporation of hydrogen before the cyclic tests modifies the dislocation structures induced by fatigue at different plastic strain amplitudes. The results of this experiment are presented first. However, since the nickel-hydrogen systems were aged several months before the NI tests, only trapped hydrogen remained in the samples. Consequently, we also performed *in-situ* ECNI on cyclically pre-strained nickel single crystal (sample A1, $\gamma_p = 2.5 \times 10^{-4}$ and sample A4, $\gamma_p = 51 \times 10^{-4}$) and the L-D results are then discussed in the following section. The tensile tests, together with the TDS and DSC measurements, were performed on un-strained aged nickel hydrogen systems and the results are analysed in the discussion section. These additional tests were conducted to evaluate the consequences of vacancies induced by hydrogen incorporation on the elastic properties of aged nickel hydrogen systems.

3. Results

3.1 Ex-situ nanoindentation on pure nickel and aged nickel-hydrogen systems

We conducted NI tests on cyclically pre-strained nickel samples with and without hydrogen. First, we performed the tests on nickel single crystal with neither hydrogen nor plastic strain for several maximum forces, F_{max}. However, the hardness H decreased with the depth of indent (an effect observed in many metals [45,57,58]) and is due to the indentation size effect. This effect can be described using models which assume that the indent develops geometrically necessary circular dislocation loops to adapt to the penetration of the indent [57,59]. Therefore, all the following NI tests were performed at F_{max} = 50 µN due to this significant

variation. The results of H and E_r are presented as a function of the plastic strain amplitudes (γ_p) in **Figures 1(a)** and **1(b)**, for pure nickel and nickel-hydrogen systems, respectively. More than 50 load-displacement tests were performed for each sample in order to obtain representative values of H and E_r. We noted a slight decrease in H with an increase in plastic strain amplitude up to $\gamma_p \sim 0.001$, then the H remained constant at 3.8 GPa for pure nickel. When the solute was charged before the cyclic tests, H was lower for a given plastic strain amplitude (3.6 GPa), a loss of 5.2%. Moreover, no particular effect of plastic strain amplitude and hydrogen incorporation on the reduced modulus (E_r) was noted, which was constant at around 160 GPa. It is important to note that the hydrogen charging of these samples was conducted just before the fatigue tests and they had been desorbed several months before the NI tests were performed. Hence, the nickel-hydrogen systems contained only hydrogen trapped deep in the dislocation structures that develop in fatigue.

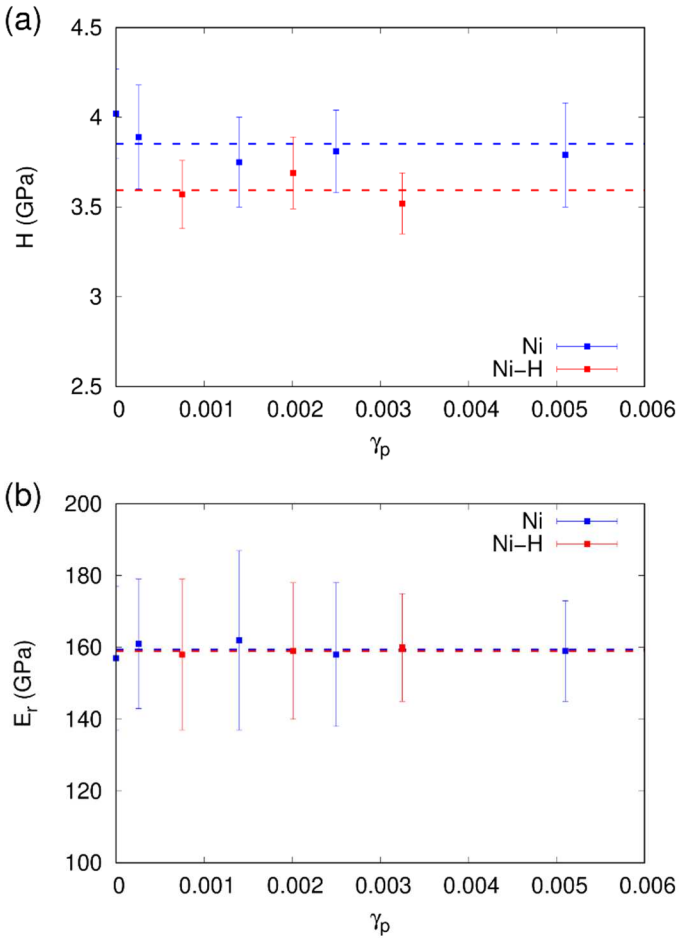

Figure 1: Hardness of pure nickel and nickel-hydrogen systems with different plastic strain amplitudes obtained at a load of 50 µN (a). The corresponding reduced modulus (b).

3.2 In-situ electrochemical nanoindentation on cyclically strained nickel single crystal

In-situ ECNI tests were also conducted on two cyclically strained nickel samples without hydrogen (one of the samples with $\gamma_p = 2.5 \times 10^{-4}$ and the other with $\gamma_p = 51 \times 10^{-4}$). The L-D results are presented in **Figures 2(a)** and **2(b)**. We observed similar behaviour for both of the cyclically pre-strained samples: when hydrogen was introduced, the maximum indentation depth was reduced compared to the tests performed under air. Then, during the NI tests under anodic polarisation (where hydrogen is desorbed from the metal), the maximum indentation depth was identical to the value obtained when the tests were carried out under air.

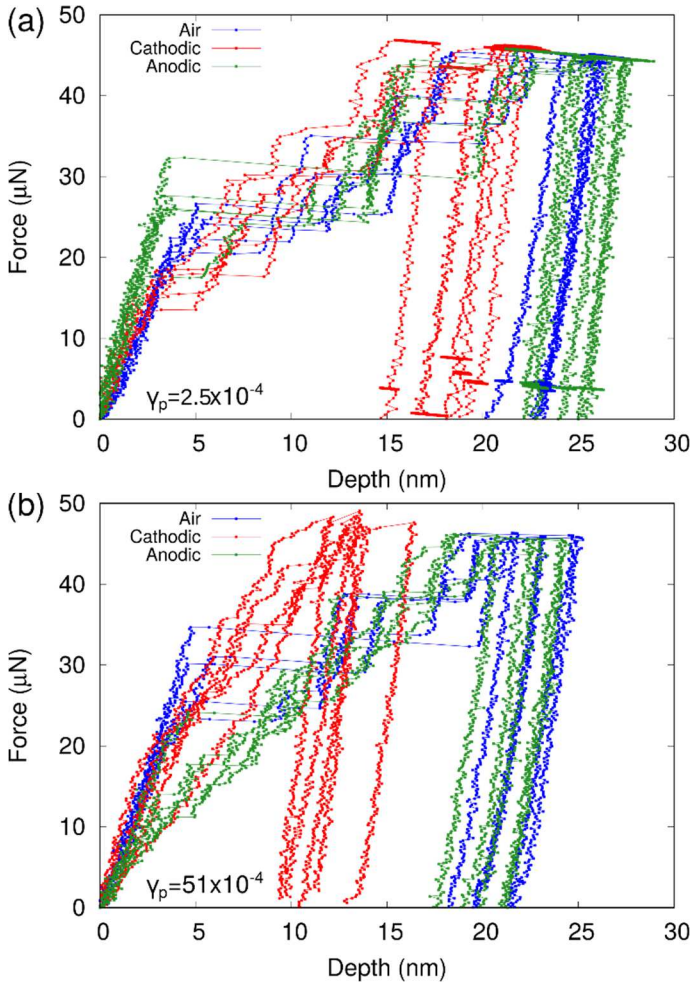

Figure 2: Load-displacement curves of *in-situ* ECNI on pre-strained nickel single crystals at $\gamma_p = 2.5 \times 10^{-4}$ (a) and $\gamma_p = 51 \times 10^{-4}$ μN (b). The blue curves represent the indents made under air, the red curves to those obtained under cathodic polarisation and the green curves those obtained under anodic polarisation.

We then evaluated the H of the metal under different conditions from these L-D curves, and the results are shown in **Table 2**. Contrary to the *ex-situ* tests (where the solute had time to desorb), a slight increase in H was noted when the samples were electrochemically charged. This increase was observed in previous studies for different metals (including nickel) and alloys [37–40,60,61]. Additional NI tests were then conducted under anodic polarisation (where the solute had been desorbed). The L-D curves for these tests almost cover the curves of the NI tests carried out in air, showing that the increase in H was only due to the incorporation of the solute in the metal. Moreover, the E_r was determined from these L-D curves, but large variations (exceeding 20%) were obtained for the same sample in the same environment.

Table 2: Hardness values with the corresponding standard deviation (GPa) under different conditions.

γ_p	Air	Cathodic	Anodic
2.5×10^{-4}	4.00 ± 0.14	6.08 ± 1.39	3.86 ± 0.23
51×10^{-4}	4.57 ± 0.31	9.94 ± 1.84	4.66 ± 0.39

To summarise the results presented in this section, hydrogen introduced before the fatigue tests led to a change in the dislocation structures, which reduced H compared with dislocation structures induced by fatigue in pure nickel single crystal: hydrogen softened the microstructures. However, when *in-situ* ECNI tests were performed on cyclically strained nickel single crystal, the solute led to an increase in H: hydrogen hardened the microstructures. These results confirm the apparent conflict, discussed in previous studies,

between the hardening of the microstructure due to the incorporation of the solute and the softening associated with the development of the microstructure induced in the presence of solute [31,32].

3.3 Vacancy contributions to the variation in the reduced modulus

Since no variation in E_r was observed in the presence of trapped hydrogen, this indicates either a recovery of the elastic properties or that hydrogen had no effect on these properties. It has been reported that the E_r of commercial Ni-201 decreases with hydrogen, while the solute can interact with others impurities in this alloy; it has also been observed that E_r tends to go back to its initial value when the solute is desorbed at room temperature for one year [34]. This behaviour implies that the degradation of the elastic properties is mostly due to mobile hydrogen, and that trapped hydrogen has only a minor effect. However, it is also well-known that hydrogen induces the formation of vacancies and vacancy clusters [53,62–64] and these defects can have a stronger impact on the elastic properties than the solute itself [51,65]; this behaviour has also been observed in other FCC alloys [66]. Thus, the behaviour of E_r should also depend on vacancy concentration.

Figure 3 presents the hydrogen concentration of an unstrained nickel-hydrogen system aged in air and determined by TDS. This figure shows that after a month of desorption in air, hydrogen could still be observed in the metal (the concentration was divided by 4 approximately). For a long hydrogen desorption time, the concentration corresponded mostly to hydrogen trapped by defects formed by hydrogen incorporation (*i.e.* vacancies and vacancy clusters).We therefore conducted tensile tests and differential scanning calorimetry of aged unstrained nickel-hydrogen systems to evaluate the concentration of vacancies and their consequences on the mechanical properties of the sample.

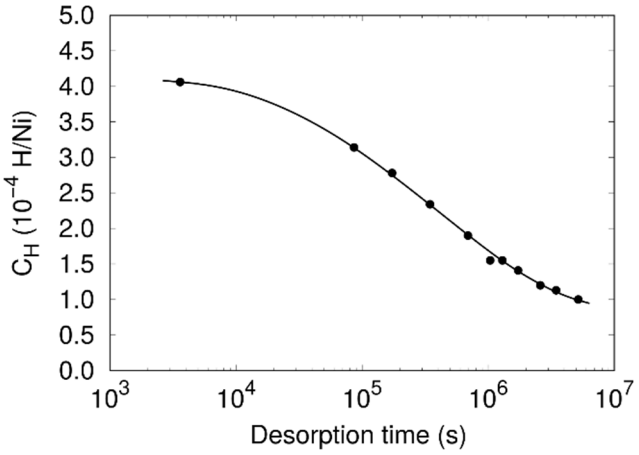

Figure 3: Hydrogen concentration in nickel-hydrogen systems as a function of desorption time at room temperature.

Figures 4(a) and **4(b)** show examples of stress-strain and heat flow of aged nickel-hydrogen systems at several hydrogen desorption times (2.6×10^3 s, 4.7×10^5 s and 2.6×10^6 s), respectively. When the hydrogen desorption time was shorter, the slope of the stress-strain increased and the stored energy of vacancies E_{Vac}^{st} (the grey area under the curves) decreased, highlighting a recovery of the elastic properties when the vacancy concentration decreased. We averaged the stored energy per vacancy concentration for at least four samples to improve the measurement. **Figure 4(c)** groups the <001> Young's modulus and vacancy concentration in aged nickel-hydrogen systems for several desorption time besides the ones shown on **Figures 4(a)** and **4(b)**. The initial value of $E_{001}(Ni-H)$ was 15% lower than that of nickel without hydrogen ($E_{001}(Ni) = 131$ GPa). This effect has been comprehensively analysed in the past and can be attributed to the formation of vacancy clusters induced by hydrogen ingress [51]. The concentration of trapped hydrogen was measured by TDS and was around 6.10^{-5} H/Ni (1 wppm) after two months of hydrogen desorption. During the desorption regime, we observed an increase in the Young's modulus, which can be correlated with a decrease in vacancy concentration. At ambient temperature, hydrogen atoms are more mobile than vacancies in nickel.

Hence, the solute desorbs from the metal and consequently the vacancies are annihilated, inducing a partial recovery of the elastic properties.

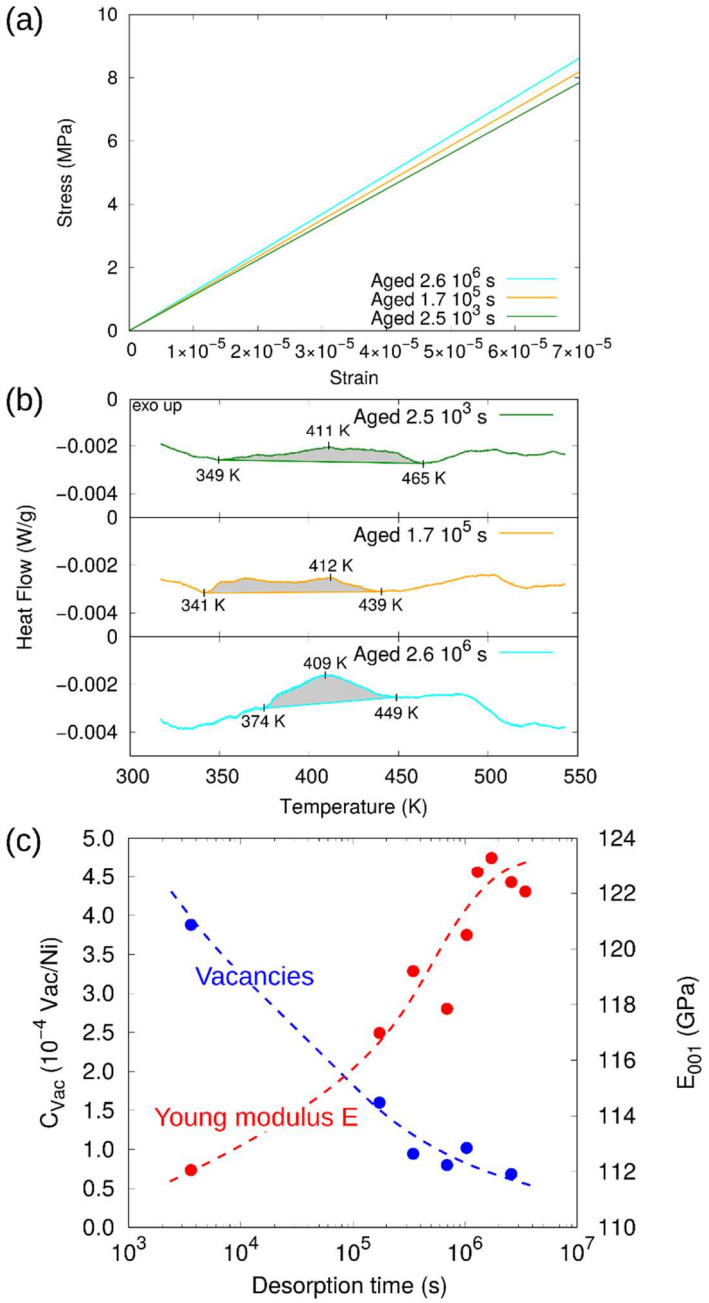

Figure 4: Stress-strain (a) and heat flow (b) in aged nickel-hydrogen systems. The concentration of vacancies obtained with DSC measurements and the <001> oriented Young's modulus is also provided for comparison (c).

4. Discussion

4.1 Impact of hydrogen on the reduced modulus

We performed NI tests on cyclically pre-strained and hydrogen pre-charged nickel single crystal to evaluate and characterise the different hardening and softening effects of a solute on the dislocation structures induced by fatigue. First, standard NI tests were performed on a reference sample (pure nickel single crystal,

without any deformation or hydrogen). Then, we chose to evaluate the consequences of hydrogen and the plastic strain amplitude at one maximum force (50 µN) since H depends on this value. We studied the consequences of hydrogen on the E_r and H of cyclically pre-strained nickel and aged nickel-hydrogen systems. No significant variation in the reduced modulus was observed between samples with or without trapped hydrogen. We then proceeded to investigate the contribution of hydrogen and hydrogen induced vacancies to the elastic properties of aged nickel-hydrogen systems. The main results were that hydrogen was desorbed as well as the vacancies and a recovery of the <001> Young's modulus was obtained when the specimens were tensile strained in an elastic regime and aged in air. In previous studies, it was observed that vacancies induced by hydrogen had a greater effect on the elastic properties of a metal than the solute itself [51]. Hence, the reduced modulus of nickel-hydrogen systems may decrease in the presence of vacancies, and could then increase up to a limit lower than the E_r of pure nickel (similar to E_{001}). However, we observed that $E_r(Ni-H) \approx E_r(Ni)$, suggesting that there are other mechanisms reducing the vacancy concentration before the NI tests. The nickel-hydrogen systems used for the NI tests were cyclically pre-strained at different plastic strain amplitudes, γ_P. Additional DSC measurements were therefore made on cyclically pre-strained nickel-hydrogen, and the results are presented on **Figure 5.** We observed that the vacancy concentration of cyclically pre-strained nickel-hydrogen systems was lower than that of the initial structure, without deformation. In other words, when the nickel-hydrogen systems were strained, the hydrogen induced vacancies and vacancy clusters were annihilated by the cyclic tests, inducing the dislocation structures presented in a previous study [31]. We use the word annihilation because less vacancies were observed with DSC. When a metal is cyclically strained, these defects are more likely used to form dislocation dipoles (see reference [67] for more details on the formation of a dislocation dipole). Moreover, a production of vacancy concentration was noted, in agreement with the results of other studies [68–70] when the plastic strain amplitude γ_P increased, but the concentration remained lower than the vacancy concentration of unstrained nickel-hydrogen systems. Hence, the E_r of cyclically strained pure nickel and aged nickel-hydrogen systems was similar (**Figure 1(b)** because the vacancy induced by hydrogen was reduced by the cyclic tests and by the desorption time.

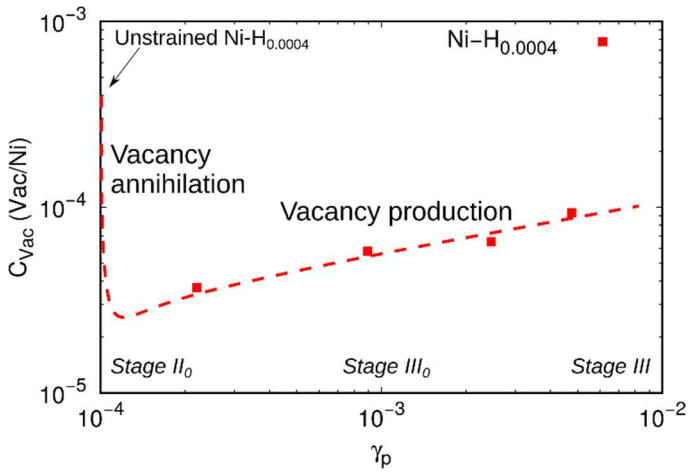

Figure 5: Vacancy concentration with the plastic strain amplitude of nickel-hydrogen systems. The different hardening stages of the cyclic tests are also provided.

4.2 Impact of hydrogen on hardness

During the standard NI tests, the H of cyclically pre-strained nickel-hydrogen specimens was lower than that of cyclically pre-strained pure nickel for all plastic strain amplitudes. Using equation (1), the H values in our study may reflect different penetration depths of the tip for a given P_{max} load. Initially, when the NI tests were carried out on cyclically pre-strained nickel, the penetration depth was higher compared to the unstrained material for a given maximum load. This induced a decrease in H because the structure had more dislocation sources, allowing the indent to penetrate more easily [71,72]. Then, when *in-situ* NI tests were carried out under electrochemical charging, a clear hardening was observed, *i.e.* the penetration depth was lower.

The hardening effect of hydrogen has been observed in pure nickel [35] and also on many metals and alloys such as ferritic stainless steel [40], dual phase steels [39] and nickel alloys [37]. Discrete dislocation dynamics (DDD) simulations may explain this hardening [42]. The authors showed that for materials with a low hydrogen diffusion coefficient (*e.g.* monocrystalline nickel), the solute accumulated around the edge components of a dislocation loop, causing a pinning effect. This pinning then induced an increase in the constraint to move the loop. This effect was observed during the *in-situ* NI tests and is equivalent to a constraint that blocks plastic flow. In the work of Girardin and Delafosse, this constraint was evaluated through experimental measurements of the solute drag with dynamic strain ageing [73]. From the different ageing peak stresses used , they expected a saturated pinning stress of around 20 MPa in pure nickel when $1.89.10^{-3}$ H/Ni (32 wppm) of hydrogen was incorporated into the metal [73]. In a previous study, the pinning effect of edge dislocations by hydrogen $\Delta\tau^{MNL}$ (for Mott-Nabarro-Labusch) was also described using a model based on the solid solution strengthening of dislocations [74–78]:

$$\Delta\tau^{MNL} = \frac{f_{max}}{b^2}\left(\frac{c_H}{2\Gamma_l}\right)^{1/2}\left(1 + 2.5\frac{w}{b}\left(\frac{2c_H\Gamma_l}{f_{max}}\right)^{1/2}\right)^{1/3} \quad (4)$$

where b is the Burgers vector (0.25 nm), f_{max} represents the maximum interaction force between solutes and dislocations, and w corresponds to the interaction distance of the solute with the dislocation. Γ_l is the line tension coefficient. The details on how to determine these values were presented in the previous study [32], and they are: 1.4×10^{-10} N, 2.5b and $0.95 \times \mu b^2/2 \times (1 - 2\nu)$, with μ and ν, the shear modulus and Poisson ratio of pure nickel. Using these values, we obtained a critical stress $\Delta\tau^{MNL}$ of 31 MPa when the hydrogen concentration was 1.89×10^{-3}, which is of the same order as the estimated 20 MPa from another study [73]. The hardening effect of hydrogen on pre-strained nickel single crystal is therefore similar to the hardening seen during DDD simulations of materials with a low diffusion coefficient containing dislocations: the solute hardens the metal in accordance with models for solid solution strengthening theory.

On the other hand, when hydrogen entered the metal before the fatigue tests, which was then aged for a few months at room temperature (desorption), a softening was obtained; this effect was also observed in Ni-201 alloy [34]. The cyclic tests reduced most of the vacancies induced by hydrogen (**Figure 4**) and the desorption time between the fatigue tests and the NI tests also allowed the lattice solute to desorb (and consequently allowed the remaining vacancies to be annihilated (**Figure 3**). Hence, only trapped hydrogen and trapped vacancies were in the nickel-hydrogen systems compared to cyclic pre-strained nickel (for both systems, there were also vacancies formed with the cyclic loadings). These vacancies segregated around the elastic field and attenuated the pinning effect of the edge component of the dislocation dipole by the solute atmosphere, as was highlighted with atomic simulations in the wall phase of cyclically strained metals in the previous study [32]. Based on our recent work on the elastic screening induced by hydrogen on nickel plasticity [26], the short-range and long-range internal stress of this phase was reduced with hydrogen, supporting the HELP (hydrogen enhanced localized plasticity) mechanism proposed to describe hydrogen embrittlement. Both effects are plausible explanations for the decrease in hardness with the addition of hydrogen in the present configuration. Moreover, this HELP mechanism could also play a role similar to the one it plays in BCC generic alloys: in a recent study, mechanical tests were performed on steels and the content of mobile and trapped hydrogen were determined. The results provide experimental proof that hydrogen trapped by dislocation plays a determinant role in the embrittlement of the alloys [79]. However, it is also important to note that compact screw dislocations control the plasticity of these alloys, whereas, in FCC alloys, dissociated edge dislocations play a more important role.

5. Conclusion

In this work, we performed NI tests on cyclically pre-strained nickel with and without hydrogen. Two antagonist processes (hardening and softening) were identified. Desorption time and cyclic tests reduced the concentration of vacancies formed by the incorporation of hydrogen. This decrease involved a recovery of the elastic properties; consequently, the reduced modulus is almost identical for pure nickel and aged nickel hydrogen systems. A decrease in hardness was observed which could be attributed to an attenuation of hydrogen in a Cottrell atmosphere due to trapped vacancies, and a reduction in the short range and long-range

internal stress in the channel phase in the presence of hydrogen. When the solute is incorporated *in-situ* electrochemically, a clear hardening was obtained, in agreement with previous studies. This effect was due to a pinning effect of the dislocations induced by the solute. Assuming this mechanism is predominant when the *in-situ* ECNI tests were performed, we evaluated the saturated pinning stress with a model for solid solution strengthening and parameters determined in a previous study. The deduced saturated pinning stress was in agreement with the results from static strain ageing in nickel single crystal.

Acknowledgements

Funding from the French Research National Agency (ANR) through the CRACKHINIT project (Contract ANR-17-CE08-0023-01) is gratefully acknowledged.

Reference

[1] R.P. Gangloff, B.P. Somerday, Gaseous Hydrogen Embrittlement of Materials in Energy Technologies, Woodhead Publisher, 2011.

[2] F. Martin, X. Feaugas, A. Oudriss, D. Tanguy, L. Briottet, J. Kittel, State of hydrogen in matter: Fundamental ad/absorption, trapping and transport mechanisms, in: C. Blanc, I. Aubert (Eds.), Mech. - Microstruct. - Corros. Couplings, Elsevier, 2019: pp. 171--197.

[3] S. Bechtle, M. Kumar, B.P. Somerday, M.E. Launey, R.O. Ritchie, Grain-boundary engineering markedly reduces susceptibility to intergranular hydrogen embrittlement in metallic materials, Acta Mater. 57 (2009) 4148–4157. https://doi.org/10.1016/j.actamat.2009.05.012.

[4] M.L. Martin, B.P. Somerday, R.O. Ritchie, P. Sofronis, I.M. Robertson, Hydrogen-induced intergranular failure in nickel revisited, Acta Mater. 60 (2012) 2739–2745. https://doi.org/10.1016/j.actamat.2012.01.040.

[5] R. Kirchheim, B. Somerday, P. Sofronis, Chemomechanical effects on the separation of interfaces occurring during fracture with emphasis on the hydrogen-iron and hydrogen-nickel system, Acta Mater. 99 (2015) 87–98. https://doi.org/10.1016/j.actamat.2015.07.057.

[6] X. Feaugas, D. Delalfosse, Chapter 9: hydrogen and crystal defects interactions: effects on plasticity and fracture, in: Mech. - Microstruct. - Corros. Couplings, 2019: pp. 199–222.

[7] S.P. Lynch, Hydrogen embrittlement phenomena and mechanisms, Corros. Rev. 30 (2012) 105–123. https://doi.org/10.1515/corrrev-2012-0502.

[8] R. Kirchheim, A. Pundt, Hydrogen in Metals, in: D.E. Laughlin, K. Hono (Eds.), Phys. Metall., 5th ed., Elsevier, Oxford, 2014: pp. 2597–2705. https://doi.org/10.1016/B978-0-444-53770-6.00025-3.

[9] I.M. Robertson, P. Sofronis, A. Nagao, M.L. Martin, S. Wang, D.W. Gross, K.E. Nygren, Hydrogen Embrittlement Understood, Metall. Mater. Trans. A Phys. Metall. Mater. Sci. 46 (2015) 2323–2341. https://doi.org/10.1007/s11661-015-2836-1.

[10] S.P. Lynch, Discussion of some recent literature on hydrogen-embrittlement mechanisms: adressing common misunderstanding, Corros. Rev. (2019). https://doi.org/10.1017/CBO9781107415324.004.

[11] Z.S. Basinski, II. Work hardening: Surface effects. Dislocation distribution in deformed copper single crystals, Discuss. Faraday Soc. 38 (1964) 93–102. https://doi.org/10.1039/DF9643800093.

[12] O.B. Pedersen, Overview no. 89 Mechanism maps for cyclic plasticity and fatigue of single phase materials, Acta Metall. Mater. 38 (1990) 1221–1239. https://doi.org/10.1016/0956-7151(90)90194-L.

[13] A.S. Argon, Mechanical properties of single phase crystalline media: deformation at low temperature, in: J.W. Cahn, P. Haasen (Eds.), Phys. Metall., North-Holland, 1996: pp. 1877--1955.

[14] P. Li, S.X. Li, Z.G. Wang, Z.F. Zhang, Fundamental factors on formation mechanism of

dislocation arrangements in cyclically deformed fcc single crystals, Prog. Mater. Sci. 56 (2011) 328–377. https://doi.org/10.1016/j.pmatsci.2010.12.001.
[15] X. Feaugas, P. Pilvin, A polycrystalline approach to the cyclic behaviour of f.c.c. alloys - Intragranular heterogeneity, Adv. Eng. Mater. 11 (2009) 703–709. https://doi.org/10.1002/adem.200900039.
[16] P.J. Woods, Low-amplitude fatigue of copper and copper-5 at. % aluminium single crystals, 1973. https://doi.org/10.1080/14786437308217440.
[17] A.T. Winter, A model for the fatigue of copper at low plastic strain amplitudes, Philos. Mag. 30 (1974) 719–738. https://doi.org/10.1080/14786437408207230.
[18] H. Haddou, M. Risbet, G. Marichal, X. Feaugas, The effects of grain size on the cyclic deformation behaviour of polycrystalline nickel, Mater. Sci. Eng. A. 379 (2004) 102–111. https://doi.org/10.1016/j.msea.2003.12.069.
[19] H. Mughrabi, Dislocation wall and cell structures and long-range internal stresses in deformed metal crystals, Acta Metall. 31 (1983) 1367–1379. https://doi.org/10.1016/0001-6160(83)90007-X.
[20] H. Mughrabi, Dislocation clustering and long-range internal stresses in monotonically and cyclically deformed metal crystals, Rev. Phys. Appliquée. 23 (1988) 367–379. https://doi.org/10.1051/rphysap:01988002304036700.
[21] N. Hansen, X. Huang, Microstructure and flow stress of polycrystals and single crystals, Acta Mater. 46 (1998) 1827–1836. https://doi.org/10.1016/S1359-6454(97)00365-0.
[22] X. Feaugas, H. Haddou, Effects of grain size on dislocation organization and internal stresses developed under tensile loading in fcc metals, Philos. Mag. 87 (2007) 989–1018. https://doi.org/10.1080/14786430601019441.
[23] A.H. Windle, G.C. Smith, The Effect of Hydrogen on the Plastic Deformation of Nickel Single Crystals, Met. Sci. J. 2 (1968) 187–191. https://doi.org/10.1179/030634568790443314.
[24] Y. Yagodzinskyy, T. Saukkonen, F. Tuomisto, S. Barannikova, L. Zuev, H. Hänninen, Effect of Hydrogen on Plastic Strain Localization in Single Crystals of Nickel and Austenitic Stainless Steel, in: B. Somerday, P. Sofronis, R. Jones (Eds.), Proc. 2008 Int. Hydrog. Conf., 2009: pp. 97–104.
[25] D. Delafosse, Hydrogen effects on the plasticity of face centred cubic (fcc) crystals, 2012. https://doi.org/10.1016/B978-0-85709-536-7.50009-X.
[26] G. Girardin, C. Huvier, D. Delafosse, X. Feaugas, Correlation between dislocation organization and slip bands: TEM and AFM investigations in hydrogen-containing nickel and nickel-chromium, Acta Mater. 91 (2015) 141–151. https://doi.org/10.1016/j.actamat.2015.03.016.
[27] I.M.A. Ghermaoui, A. Oudriss, A. Metsue, R. Milet, K. Madani, X. Feaugas, Multiscale analysis of hydrogen-induced softening in f.c.c. nickel single crystals oriented for multiple-slips: elastic screening effect, Sci. Rep. 9 (2019). https://doi.org/10.1038/s41598-019-49420-6.
[28] T. Boniszewski, G.C. Smith, The influence of hydrogen on the plastic deformation ductility, and fracture of nickel in tension, Acta Metall. 11 (1963) 165–178. https://doi.org/10.1016/0001-6160(63)90209-8.
[29] S.K. Lawrence, Y. Yagodzinskyy, H. Hänninen, E. Korhonen, F. Tuomisto, Z.D. Harris, B.P. Somerday, Effects of grain size and deformation temperature on hydrogen-enhanced vacancy formation in Ni alloys, Acta Mater. 128 (2017) 218–226. https://doi.org/10.1016/j.actamat.2017.02.016.
[30] T. Magnin, C. Bosch, K. Wolski, D. Delafosse, Cyclic plastic deformation behaviour of Ni single crystals oriented for single slip as a function of hydrogen content, Mater. Sci. Eng. A. 314 (2001) 7–11. https://doi.org/10.1016/S0921-5093(00)01920-1.
[31] G. Hachet, A. Oudriss, A. Barnoush, R. Milet, D. Wan, A. Metsue, X. Feaugas, The influence

of hydrogen on cyclic plasticity of <001> oriented nickel single crystal. Part I: Dislocation organisations and internal stresses, Int. J. Plast. 126 (2020) 102611. https://doi.org/10.1016/j.ijplas.2019.09.017.
[32] G. Hachet, A. Metsue, A. Oudriss, X. Feaugas, The influence of hydrogen on cyclic plasticity of <001> oriented nickel single crystal. Part II: Stability of edge dislocation dipoles, Int. J. Plast. 129 (2020) 102667. https://doi.org/10.1016/j.ijplas.2020.102667.
[33] G.M. Castelluccio, C.B. Geller, D.L. McDowell, A rationale for modeling hydrogen effects on plastic deformation across scales in FCC metals, Int. J. Plast. 111 (2018) 72–84. https://doi.org/10.1016/j.ijplas.2018.07.009.
[34] S.K. Lawrence, B.P. Somerday, R.A. Karnesky, Elastic Property Dependence on Mobile and Trapped Hydrogen in Ni-201, Jom. 69 (2017) 45–50. https://doi.org/10.1007/s11837-016-2157-x.
[35] A. Barnoush, H. Vehoff, Recent developments in the study of hydrogen embrittlement: Hydrogen effect on dislocation nucleation, Acta Mater. 58 (2010) 5274–5285. https://doi.org/10.1016/j.actamat.2010.05.057.
[36] A. Barnoush, Correlation between dislocation density and nanomechanical response during nanoindentation, Acta Mater. 60 (2012) 1268–1277. https://doi.org/10.1016/j.actamat.2011.11.034.
[37] G. Stenerud, R. Johnsen, J.S. Olsen, J. He, A. Barnoush, Effect of hydrogen on dislocation nucleation in alloy 718, Int. J. Hydrogen Energy. 42 (2017) 15933–15942. https://doi.org/10.1016/j.ijhydene.2017.04.290.
[38] D. Wang, X. Lu, Y. Deng, X. Guo, A. Barnoush, Effect of hydrogen on nanomechanical properties in Fe-22Mn-0.6C TWIP steel revealed by in-situ electrochemical nanoindentation, Acta Mater. 166 (2019) 618–629. https://doi.org/10.1016/j.actamat.2018.12.055.
[39] T. Depover, T. Hajilou, D. Wan, D. Wang, A. Barnoush, K. Verbeken, Assessment of the potential of hydrogen plasma charging as compared to conventional electrochemical hydrogen charging on dual phase steel, Mater. Sci. Eng. A. 754 (2019) 613–621. https://doi.org/10.1016/j.msea.2019.03.097.
[40] J. Kim, C.C. Tasan, Microstructural and micro-mechanical characterization during hydrogen charging: An in situ scanning electron microscopy study, Int. J. Hydrogen Energy. 44 (2019) 6333–6343. https://doi.org/10.1016/j.ijhydene.2018.10.128.
[41] J. Song, W.A. Curtin, Mechanisms of hydrogen-enhanced localized plasticity: An atomistic study using α-Fe as a model system, Acta Mater. 68 (2014) 61–69. https://doi.org/10.1016/j.actamat.2014.01.008.
[42] Y. Gu, J.A. El-Awady, Quantifying the effect of hydrogen on dislocation dynamics: A three-dimensional discrete dislocation dynamics framework, J. Mech. Phys. Solids. 112 (2018) 491–507. https://doi.org/10.1016/j.jmps.2018.01.006.
[43] T. Hajilou, Y. Deng, B.R. Rogne, N. Kheradmand, A. Barnoush, In situ electrochemical microcantilever bending test: A new insight into hydrogen enhanced cracking, Scr. Mater. 132 (2017) 17–21. https://doi.org/10.1016/j.scriptamat.2017.01.019.
[44] T. Hajilou, M.S.B. Hope, A.H. Zavieh, N. Kheradmand, R. Johnsen, A. Barnoush, In situ small-scale hydrogen embrittlement testing made easy: An electrolyte for preserving surface integrity at nano-scale during hydrogen charging, Int. J. Hydrogen Energy. 43 (2018) 12516–12529. https://doi.org/10.1016/j.ijhydene.2018.04.168.
[45] A. Barnoush, Hydrogen embrittlement, revisited by in situ electrochemical nanoindentation, Universität des Saarlandes, 2007.
[46] D.M. Ebenstein, K.J. Wahl, A comparison of JKR-based methods to analyze quasi-static and dynamic indentation force curves, J. Colloid Interface Sci. 298 (2006) 652–662. https://doi.org/10.1016/j.jcis.2005.12.062.
[47] W.C. Oliver, G.M. Pharr, Measurement of hardness and elastic modulus by instrumented

indentation: Advances in understanding and refinements to methodology, J. Mater. Res. 19 (2004) 3–20. https://doi.org/10.1557/jmr.2004.19.1.3.
[48] W.C. Oliver, G.M. Pharr, An Improved technique for Determining Hardness and Elastic Modulus using Load and Displacement Sensing Indentation Experiments, J. Mater. Res. 7 (1992) 1564–1583. https://doi.org/10.1557/JMR.1992.1564.
[49] J.J. Vlassak, W.D. Nix, Measuring the elastic properties of anisotropic materials by means of indentation experiments, J. Mech. Phys. Solids. 42 (1994) 1223–1245. https://doi.org/10.1016/0022-5096(94)90033-7.
[50] J. Li, A. Oudriss, A. Metsue, J. Bouhattate, X. Feaugas, Anisotropy of hydrogen diffusion in nickel single crystals: The effects of self-stress and hydrogen concentration on diffusion, Sci. Rep. 7 (2017) 1–9. https://doi.org/10.1038/srep45041.
[51] G. Hachet, A. Metsue, A. Oudriss, X. Feaugas, Influence of hydrogen on the elastic properties of nickel single crystal: A numerical and experimental investigation, Acta Mater. 148 (2018). https://doi.org/10.1016/j.actamat.2018.01.056.
[52] A. Oudriss, X. Feaugas, Length scales and scaling laws for dislocation cells developed during monotonic deformation of (001) nickel single crystal, Int. J. Plast. 78 (2016) 187–202. https://doi.org/10.1016/j.ijplas.2015.11.003.
[53] A. Oudriss, J. Creus, J. Bouhattate, E. Conforto, C. Berziou, C. Savall, X. Feaugas, Grain size and grain-boundary effects on diffusion and trapping of hydrogen in pure nickel, Acta Mater. 60 (2012) 6814–6828. https://doi.org/10.1016/j.actamat.2012.09.004.
[54] D. Guedes, A. Oudriss, S. Frappart, G. Courlit, S. Cohendoz, P. Girault, J. Creus, J. Bouhattate, A. Metsue, F. Thebault, L. Delattre, D. Koschel, X. Feaugas, The influence of hydrostatic stress states on the hydrogen solubility in martensitic steels, Scr. Mater. 84–85 (2014) 23–26. https://doi.org/10.1016/j.scriptamat.2014.04.006.
[55] D. Setman, E. Schafler, E. Korznikova, M.J. Zehetbauer, The presence and nature of vacancy type defects in nanometals detained by severe plastic deformation, Mater. Sci. Eng. A. 493 (2008) 116–122. https://doi.org/10.1016/j.msea.2007.06.093.
[56] A. Metsue, A. Oudriss, J. Bouhattate, X. Feaugas, Contribution of the entropy on the thermodynamic equilibrium of vacancies in nickel, J. Chem. Phys. 140 (2014). https://doi.org/10.1063/1.4867543.
[57] W.D. Nix, H. Gao, Indentation size effects in crystalline materials: A law for strain gradient plasticity, J. Mech. Phys. Solids. 46 (1998) 411–425. https://doi.org/10.1016/S0022-5096(97)00086-0.
[58] Z. Wang, Influences of sample preparation on the indentation size effect and nanoindentation pop-in on nickel, University of Tennessee, 2012.
[59] J.G. Swadener, E.P. George, G.M. Pharr, The correlation of the indentation size effect measured with indenters of various shapes, J. Mech. Phys. Solids. 50 (2002) 681–694. https://doi.org/10.1016/S0022-5096(01)00103-X.
[60] A. Barnoush, H. Vehoff, Electrochemical nanoindentation: A new approach to probe hydrogen/deformation interaction, Scr. Mater. 55 (2006) 195–198. https://doi.org/10.1016/j.scriptamat.2006.03.041.
[61] X. Lu, Y. Ma, M. Zamanzade, Y. Deng, D. Wang, W. Bleck, W.W. Song, A. Barnoush, Insight into hydrogen effect on a duplex medium-Mn steel revealed by in-situ nanoindentation test, Int. J. Hydrogen Energy. 44 (2019) 20545–20551. https://doi.org/10.1016/j.ijhydene.2019.04.290.
[62] N.Z. Carr, R.B. McLellan, Hydrogen-vacancy interactions in Ni-H solid solutions, J. Phys. Chem. Solids. 67 (2006) 1797–1802. https://doi.org/10.1016/j.jpcs.2006.02.021.
[63] S. Harada, S. Yokota, Y. Ishii, Y. Shizuku, M. Kanazawa, Y. Fukai, A relation between the vacancy concentration and hydrogen concentration in the Ni-H, Co-H and Pd-H systems, J. Alloys Compd. 404–406 (2005) 247–251. https://doi.org/10.1016/j.jallcom.2005.02.077.

[64] Y. Fukai, Formation of superabundant vacancies in M-H alloys and some of its consequences: A review, J. Alloys Compd. 356–357 (2003) 263–269. https://doi.org/10.1016/S0925-8388(02)01269-0.
[65] G. Hachet, J. Li, A.M.M. Hallil, A. Metsue, A. Oudriss, J. Bouhattate, X. Feaugas, A multi-scale analysis of the different interactions between defects and hydrogen: A review on the contribution of the elastic fields, Eng. Fract. Mech. 218 (2019) 1–10. https://doi.org/10.1016/j.engfracmech.2019.106621.
[66] M. Zamanzade, G. Hasemann, C. Motz, M. Krüger, A. Barnoush, Vacancy effects on the mechanical behavior of B2-FeAl intermetallics, Mater. Sci. Eng. A. 712 (2018) 88–96. https://doi.org/10.1016/j.msea.2017.11.054.
[67] C. Erel, G. Po, T. Crosby, N. Ghoniem, Generation and interaction mechanisms of prismatic dislocation loops in FCC metals, Comput. Mater. Sci. 140 (2017) 32–46. https://doi.org/10.1016/j.commatsci.2017.07.043.
[68] U. Essmann, U. Gösele, H. Mughrabi, A model of extrusions and intrusions in fatigued metals I. Point-defect production and the growth of extrusions, Philos. Mag. A Phys. Condens. Matter, Struct. Defects Mech. Prop. 44 (1981) 405–426. https://doi.org/10.1080/01418618108239541.
[69] J. Polák, Resistivity of fatigued copper single crystals, Mater. Sci. Eng. 89 (1987) 35–43. https://doi.org/10.1016/0025-5416(87)90247-3.
[70] J. Man, K. Obrtlík, J. Polák, Extrusions and intrusions in fatigued metals. Part 1. State of the art and history, Philos. Mag. 89 (2009) 1295–1336. https://doi.org/10.1080/14786430902917616.
[71] H. Bei, Y.Z. Xia, R.I. Barabash, Y.F. Gao, A tale of two mechanisms: Strain-softening versus strain-hardening in single crystals under small stressed volumes, Scr. Mater. 110 (2016) 48–52. https://doi.org/10.1016/j.scriptamat.2015.07.043.
[72] Y. Gao, H. Bei, Strength statistics of single crystals and metallic glasses under small stressed volumes, Prog. Mater. Sci. 82 (2016) 118–150. https://doi.org/10.1016/j.pmatsci.2016.05.002.
[73] G. Girardin, D. Delafosse, Measurement of the saturated dislocation pinning force in hydrogenated nickel and nickel base alloys, Scr. Mater. 51 (2004) 1177–1181. https://doi.org/10.1016/j.scriptamat.2004.07.012.
[74] R. Labusch, A Statistical Theory of Solid Solution Hardening, Phys. Status Solidi. 41 (1970) 659–669. https://doi.org/10.1002/pssb.19700410221.
[75] J.W. Cahn, P. Haasen, Physical Metallurgy, 4th ed., North-Holland, 1996.
[76] S. Patinet, L. Proville, Depinning transition for a screw dislocation in a model solid solution, Phys. Rev. B - Condens. Matter Mater. Phys. 78 (2008) 1–9. https://doi.org/10.1103/PhysRevB.78.104109.
[77] J. Friedel, Dislocations, Pergramon Press, 1964.
[78] R.L. Fleischer, Substitutional solution hardening, Acta Metall. 11 (1963) 203–209. https://doi.org/10.1016/0001-6160(63)90213-X.
[79] T. Depover, K. Verbeken, The detrimental effect of hydrogen at dislocations on the hydrogen embrittlement susceptibility of Fe-C-X alloys: An experimental proof of the HELP mechanism, Int. J. Hydrogen Energy. 43 (2018) 3050–3061. https://doi.org/10.1016/j.ijhydene.2017.12.109.